Vβ4$^+$ T Cells Promote Clearance of Infection in Murine Pulmonary Histoplasmosis

Francisco J. Gomez, Judith A. Cain, Reta Gibbons, Ruth Allendoerfer, and George S. Deepe, Jr.
Division of Infectious Diseases, Department of Medicine, University of Cincinnati, Cincinnati, Ohio 45267-0560

Abstract

T cells are essential for controlling infection with *Histoplasma capsulatum*. Because the T cell receptor is vital for transducing the biological activities of these cells, we sought to determine if exposure to this fungus induced an alteration in the Vβ repertoire in lungs of C57BL/6 mice infected intranasally. Vβ2$^+$ cells were elevated on day 3 after infection; Vβ4$^+$ cells were higher than controls on days 7, 10, and 14 after infection. Vβ10$^+$ cells were increased on days 14 and 21, and Vβ11$^+$ exceeded controls only on day 14. We investigated the clonality and function of Vβ4$^+$ cells because their expansion transpired during the critical time of infection, that is, when cellular immunity is activated. Sequence analysis demonstrated preferential use of a restricted set of sequences in the complementarity-determining region 3. Elimination of Vβ4$^+$ cells from mice impaired their ability to resolve infection. In contrast, depletion of Vβ7$^+$ cells, the abundance of which was similar to that of Vβ4$^+$, did not alter elimination of the fungus. The identification of clonotypes of Vβ4$^+$ cells suggests that a few antigenic determinants may drive proliferation of this subset, which is necessary for optimal clearance. (*J. Clin. Invest.* 1998. 102:984–995.) Key words: *Histoplasma capsulatum* • receptor, antigen, T cell, α/β • T lymphocytes subsets • polymerase chain reaction • immunity, cellular

Introduction

Histoplasmosis is a deep mycosis that is manifest in higher mammals and humans. Infection is initiated by inhalation of mycelial fragments and microconidia. After settling into lungs, the saprobic phase converts into yeasts, and these forms are engulfed by alveolar macrophages and reside within the endosomal compartment of these cells (1–3). Control and clearance of the fungus is critically dependent on an intact cellular immune system (4, 5).

Experimental and clinical observations connote the central role of T cells in host resistance to this fungus. Thus, mice congenitally deficient in, or experimentally depleted of T cells are much more susceptible to infection with *Histoplasma capsulatum* (Hc)[1] as compared to immunocompetent controls (6, 7). Similarly, patients with T cell dysfunction caused by immunosuppressive therapy or HIV infection exhibit a higher incidence of disseminated histoplasmosis (8–10).

The mechanisms T cells use to confer resistance to the fungus are not completely understood. It is known that T cells recognize Hc antigens presented by accessory cells, become activated, and secrete cytokines that arm macrophages to exert fungistatic and/or fungicidal activity (11–14). T cells are exceptionally heterogeneous, and can be categorized on the basis of functional or phenotypic differences: Th1 versus Th2, naive, activated or memory, CD4 versus CD8, α/β versus γ/δ T cell receptor (TCR) chains, and by their unique, clonotypic TCR. Information regarding the contribution of functional and phenotypic subpopulations to host defenses against Hc are just emerging.

Systematic deletion of a subpopulation of T cells has provided substantial insight into the influence of T cells on the course of infection. Mice depleted of CD4$^+$ T cells succumb to a sublethal inoculum with Hc yeasts (7). Conversely, CD8$^+$-depleted mice do not exhibit higher mortality to Hc infection than controls, but do have a delayed clearance of the fungus from tissues (9).

Among the molecules that decorate the surface of T cells, the TCR stands as the most heterogeneous, with the potential of 10^{15} clonotypes. The TCR interacts with the vast array of antigenic peptides present in the groove of MHC molecules. It is one of the key molecules in recognition of self from non-self, and embodies the specificity of the immune system (15–17). The most abundant and best studied TCR family is composed of two chains, α and β. The diversity of the TCR is generated by somatic recombination between one of variable (V) region genes, one of the junctional (J) region genes, a constant (C) region gene in the α chain, and V, J, and a diversity (D) and C regions in the β chain (18). Additional variability in the sequence is generated by the random loss or addition of nucleotides at the junction sites, the N and P sequences. Every α/β–bearing T cell possesses one and only one particular TCR. It is thought that each particular TCR recognizes one or at most a few antigenic peptides from an antigen (18).

In these experiments, we quantified the Vβ TCR repertoire in lungs of mice during the course of primary infection with Hc. This organ was selected because it is the portal of entry. We sought to identify Vβ families that become expanded in response to infection. We then altered the TCR repertoire by eliminating the T cell subpopulation bearing the expanded Vβ family and examined the impact of this maneuver on the course of the infection.

Address correspondence to George S. Deepe, Jr., Infectious Diseases Division, College of Medicine, 231 Bethesda Ave. ML 560, Cincinnati, OH 45267-0560. Phone: 513-558-4704; FAX: 513-558-2089; E-mail: deepegs@email.uc.edu

Received for publication 2 February 1998 and accepted in revised form 14 July 1998.

J. Clin. Invest.

0021-9738/98/09/0984/12 $2.00
Volume 102, Number 5, September 1998, 984–995
http://www.jci.org

1. *Abbreviations used in this paper:* CDR3, complementarity-determining region 3; Hc, *Histoplasma capsulatum*; i.p., intraperitoneally; Rdi, relative intensity index; TCR, T cell receptor.

Methods

Mice. 6-wk-old male C57BL/6 mice were purchased from Jackson Laboratories (Bar Harbor, ME). Athymic nude mice (nu/nu) were purchased from National Cancer Institute and housed under standard laboratory conditions.

Preparation and infection of mice with Hc yeasts. Hc strain G217B was prepared as previously described (19). Mice were lightly anesthetized with methoxyflurane (Mallinckrodt Veterinary, Inc., Mundelein, IL) and inoculated intranasally with a sublethal (2.5×10^6) dose of yeasts.

Preparation of monoclonal antibodies (mAb). Hybridoma cell lines KT4 (anti-Vβ4 chain of murine TCR) and TR3-10 (anti-Vβ7) were kindly provided by G. Fathman (Stanford University, Stanford, CA). Ascites were prepared in nude mice, fluid was collected, and filter sterilized. The amount of mAb was quantified by ELISA using rat IgG as a standard. mAb was diluted to a working concentration (1.6 mg/ml) in HBSS.

In vivo depletion of Vβ subpopulations. Groups of mice were injected intraperitoneally with KT4, TR3-10 mAb, or rat IgG as a control. 300 μg of mAb or an equal amount of rat IgG were administered intraperitoneally on days −7, −3, and on the day of infection. Some groups of mice were given 300 μg of Ab twice a week thereafter.

RNA preparation and cDNA synthesis. Groups of six mice were infected with Hc. Uninfected, age-matched littermates were used as controls. Animals were killed on days 3, 7, 10, 14, and 21 after infection. Lungs were flushed of circulating cells by injection of 10–20 ml of HBSS into the right ventricle. Total RNA was extracted from lungs by homogenization in 4 ml of RNAzol (BIOTECKX, Friendswood, TX). RNA was ethanol precipitated, resuspended in RNAse-free water, and quantified by OD260. Samples were frozen at −70°C until used. Single strand cDNA was synthesized from 6 μg of total RNA using a Cβ1 antisense primer (Fig. 1) in the presence of AMV reverse transcriptase (Promega, Madison, WI) according to the manufacturer's instructions in a final reaction volume of 60 μl. 1 μl aliquots were used as templates in subsequent PCR reactions.

Amplification of cDNA for Vβ families. PCR was performed in 25 μl reactions with 1.25 U of Taq Polymerase (Promega), 1.5 mM $MgCl_2$, 200 μM of each dNTPs (Pharmacia Biotech, Piscataway, NJ), and each sense and antisense primer at a final concentration of 1 μM (20). Vβ primers and nomenclature were identical to those previously published (21). Cycling conditions were 94°C for 45 s, 59°C for 45 s, and 72°C for 60 s in a 9600 Thermocycler (Perkin Elmer Corp., Norwalk, CN). Preliminary studies were performed to determine the number of cycles necessary to produce visible signal before saturation. We incubated 1 μl of each cDNA sample with a Cβ2 antisense primer and Cβ1 sense primer (Fig. 1). The expected product was a 360-bp fragment from the constant region of TCR β chain. Reactions were incubated for 26, 28, 30, 32, and 34 cycles. 5 μl of each PCR amplification were electrophoresed in 1% agarose gels and stained with ethidium bromide. The log phase of PCR amplification was established by visual inspection of the gels. Subsequently, 1 μl of cDNA was used as a template in 20 parallel reactions using a Cβ2 antisense primer and each of 20 different Vβ-specific sense primers. A positive control was run using Cβ1 sense and Cβ2 antisense primers, and a negative control using the same primers without cDNA template. The cycling conditions were the same as stated above for the number of cycles determined for each cDNA template.

Southern blot of Vβ PCR products. 5 μl of each PCR reaction were electrophoresed into 1% agarose gels and blotted onto positively charged nylon membranes (Boehringer Mannheim, Indianapolis, IN) by alkaline transfer. Blots were hybridized with a digoxigenin- (GENIUS System®, Boehringer Mannheim) labeled DNA probe specific for the 360-bp Cβ region present in every Vβ PCR product. Filters were washed with 0.2% SSC containing 0.1% SDS at 65°C. Blots were then incubated with alkaline phosphatase-conjugated anti-digoxigenin Fab (GENIUS system®, Boehringer Mannheim), and washed. Chemiluminescence substrate Lumiphos® (Boehringer Mannheim) was added and blots were exposed to X-ray film for 5–10 min. Bands were quantified by densitometry. The relative intensity index (Rdi) for each Vβ product was computed by the formula:

$$Rd(V\beta_i) = \frac{V\beta_i}{\sum_{i=1}^{i=20} V\beta_i}$$

where $V\beta_i$ represents the pixel density of each Vβ family, and the denominator denotes the sum of the densities of all 20 Vβ specific products. The relative index calculation normalizes for variation in the efficiency of transfer, hybridization, and time of exposure to the X-ray film.

Flow cytometry analysis. Groups of uninfected controls or mice infected for 10 d with Hc were killed and lungs removed. Single cell suspensions were prepared by teasing the organs apart in RPMI plus 10% FBS, and mincing the fragments through progressively thinner needles. The material was filtered through 60 mm nylon mesh. Mononuclear cells were isolated by 600 *g* centrifugation in a discontinuous 40–70% percoll gradient. Lymphocytes were further enriched by adherence of the cell suspension to tissue culture plates for 1 h at 37°C in 5% CO_2. The non-adherent population was recovered and quantified in a hemocytometer. In uninfected controls, cells from three mice were pooled to obtain sufficient numbers of cells. A minimum of 10^4 cells per tube were incubated with saturating concentrations of biotin-labeled anti-Vβ4, -Vβ10, -Vβ11, or -Vβ5 mAb (PharMingen, San Diego, CA) for 30 min at 4°C, and washed three times. Cells were then exposed to avidin-phycoerythrin for 30 min at 4°C and washed an additional three times. Total T cells were identified using fluorescein-conjugated anti–Thy-1.2 mAb. Analysis was performed on a Coulter Epics XL Flow Cytometer (Coulter Corp., Miami, FL). As a control, cells were incubated with isotype-matched irrelevant mAb. The results were calculated as number of $V\beta^+$ cells minus background divided by number of Thy-1^+ cells minus background.

Sequence analysis. Vβ4 PCR products amplified from lungs of control mice as well as mice 7, 10, and 14 d after infection were reamplified using the Vβ4 specific sense primer and a nested Cβ3 antisense primer (Fig. 1). Three to five samples per group were studied. The resulting PCR products were gel purified and cloned into PCR2.1® (Invitrogen, La Jolla, CA) vector. Random colonies were picked, and the sequence across the complementarity-determining region 3 (CDR3) was determined.

In uninfected animals, the quantity of $V\beta4^+$ PCR product was exceedingly low, and after ligation and transformation, we obtained many colonies that did not contain plasmids with the Vβ4 insert. To distinguish legitimate $V\beta4^+$ clones, we plated replicas of the bacterial plates onto nylon filters (Boehringer Mannheim) and hybridized them with a 360-bp Cβ gene fragment labeled with γ-^{32}P. After wash-

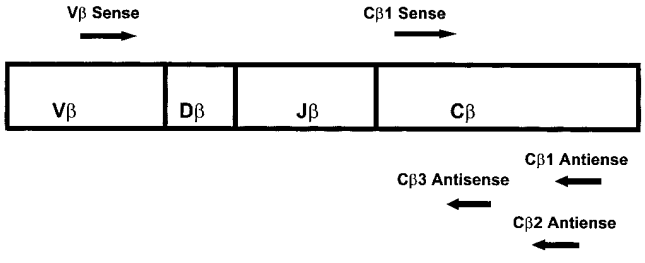

Figure 1. DNA oligonucleotide primers used for reverse transcription and PCR amplification. The primer sequences (5′-3′) and position relative to the Cβ region are: Cβ1 antisense, ACAGTCTGCTCGGCCCCAGGC, bases 380–360; Cβ2 antisense, CCCCAGGCCTCTGCACTGATG, bases 367–347; Cβ3 antisense, AAGCCCCTGGCCAAGCACACG, bases 106–86; Cβ1 sense, GGATCTGAGAAATGTGACTCC, bases 2–22.

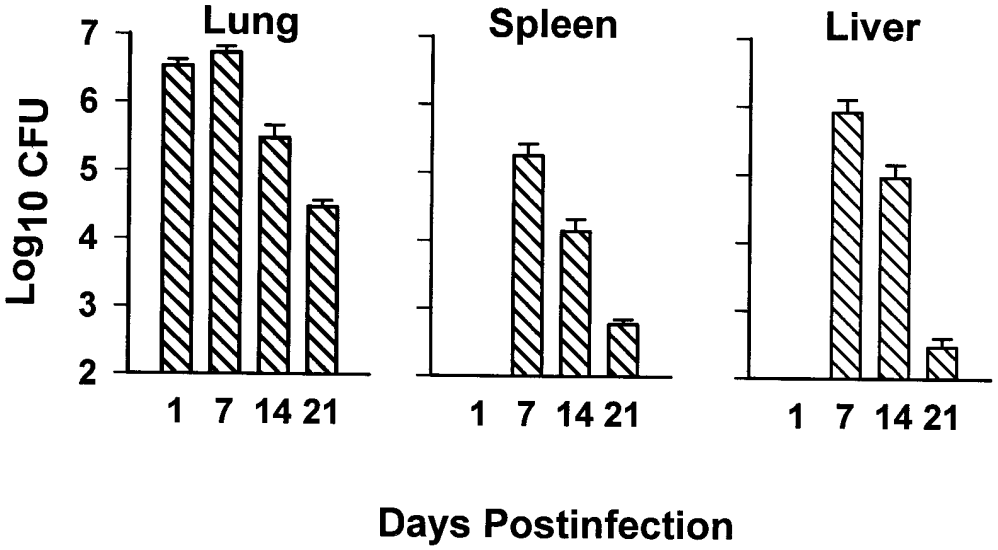

Figure 2. Fungal burden in murine pulmonary histoplasmosis. C57BL/6 mice were inoculated intranasally with 2.5×10^6 Hc yeasts. Mice were killed at days 1, 7, 14, and 21 after infection, and organs were homogenized in 10 ml of HBSS. Dilutions were plated onto blood agar plates, and CFU enumerated. Results are expressed as Log10 CFU per organ. Each bar represents the average±SEM of six mice per time point. The limit of detection was 100 CFU.

ing and autoradiography, Vβ4$^+$ containing clones were picked from the replicas and sequenced.

Quantitative organ cultures. Cultures of organs for Hc were performed as previously described (7, 19). Results were expressed as $\log_{10}$ CFU/organ.

IFN-γ measurements. Lungs of mice infected with Hc for 7, 14, or 21 d were homogenized in 10 ml of HBSS as described in quantitative organ cultures above. Concentration of IFN-γ were determined using an antigen-capture ELISA (Endogen, Cambridge, MA). The mean±SEM of triplicate samples were expressed as pg/ml of homogenate.

Statistics. Results were analyzed using SigmaStat® software package (Jandel Scientific, San Rafael, CA). Student's *t* test was used to compare two groups or one-way ANOVA was used to compare more than two groups. Dunnet's correction was used for multiple comparisons against a control group. If the data did not distribute normally, a rank sum test was used to compare two groups.

Results

Vβ Repertoire in lungs of mice infected with Hc. The course of infection, as measured by fungal burden, in mice infected intranasally with 2.5×10^6 Hc yeasts is shown in Fig. 2. Dissemination of infection beyond the lungs was detected on day 7. Recovery of Hc CFU in lungs, spleens, and livers is maximum on this day and declines thereafter. Subsequently, lungs from mice infected with the same inoculum of Hc were excised and RNA extracted on days 3, 7, 10, 14, and 21 postinfection lungs. As a control, lungs were removed from a group of uninfected, age-matched littermates. cDNA from each lung was subjected to PCR using Vβ specific primers. The amplified products were analyzed by Southern blot using a Cβ probe. A representative Southern blot is illustrated in Fig. 3.

The autoradiographs from each mouse were densitometrically quantified and data computed as stated in Methods. The relative density index (mean±SEM) of lungs from six mice per group was calculated and compared to the control group. The profiles of Vβ expression are shown in Fig. 4. Vβ2 was significantly higher than controls at day 3 after infection ($P < 0.02$). Vβ4 exceeded controls on days 7, 10 and 14 ($P < 0.01$), and expression of Vβ11 was greater than controls on day 14 only ($P < 0.01$). On days 14 and 21, Vβ10 expression exceeded controls ($P < 0.04$). When the data for each Vβ family was ana-

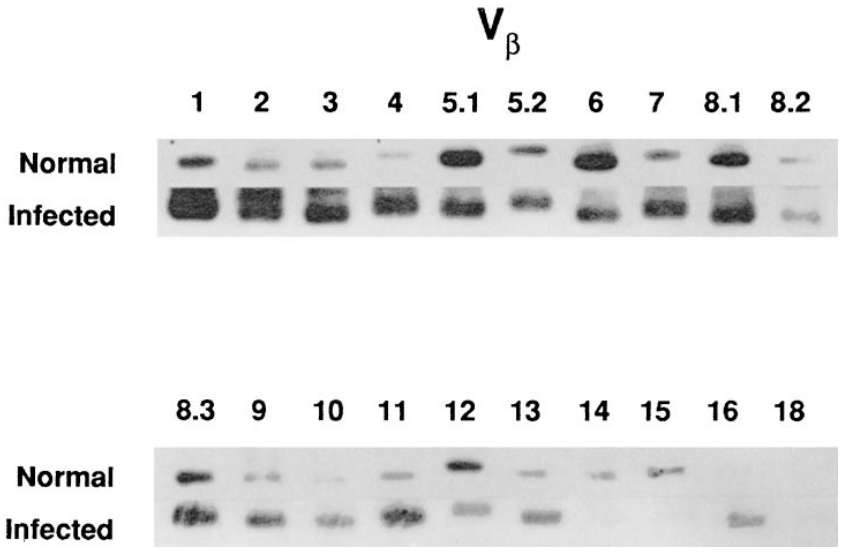

Figure 3. Southern blot of Vβ PCR products. Total RNA was extracted from mice 10 d after infection with Hc or from uninfected controls. RNA was reverse transcribed using Cβ1 antisense primer and used as template in 20 parallel PCR reactions using 20 Vβ specific sense primers and a common Cβ2 antisense primer. 5 μl of each reaction were electrophoresed in 1% agarose gels and transferred onto nylon membranes. Blots were hybridized with a Cβ specific probe, and bands were visualized by chemiluminescence. A representative blot is shown. *Normal* and *infected* designate an uninfected control mouse and a mouse infected for 10 d, respectively.

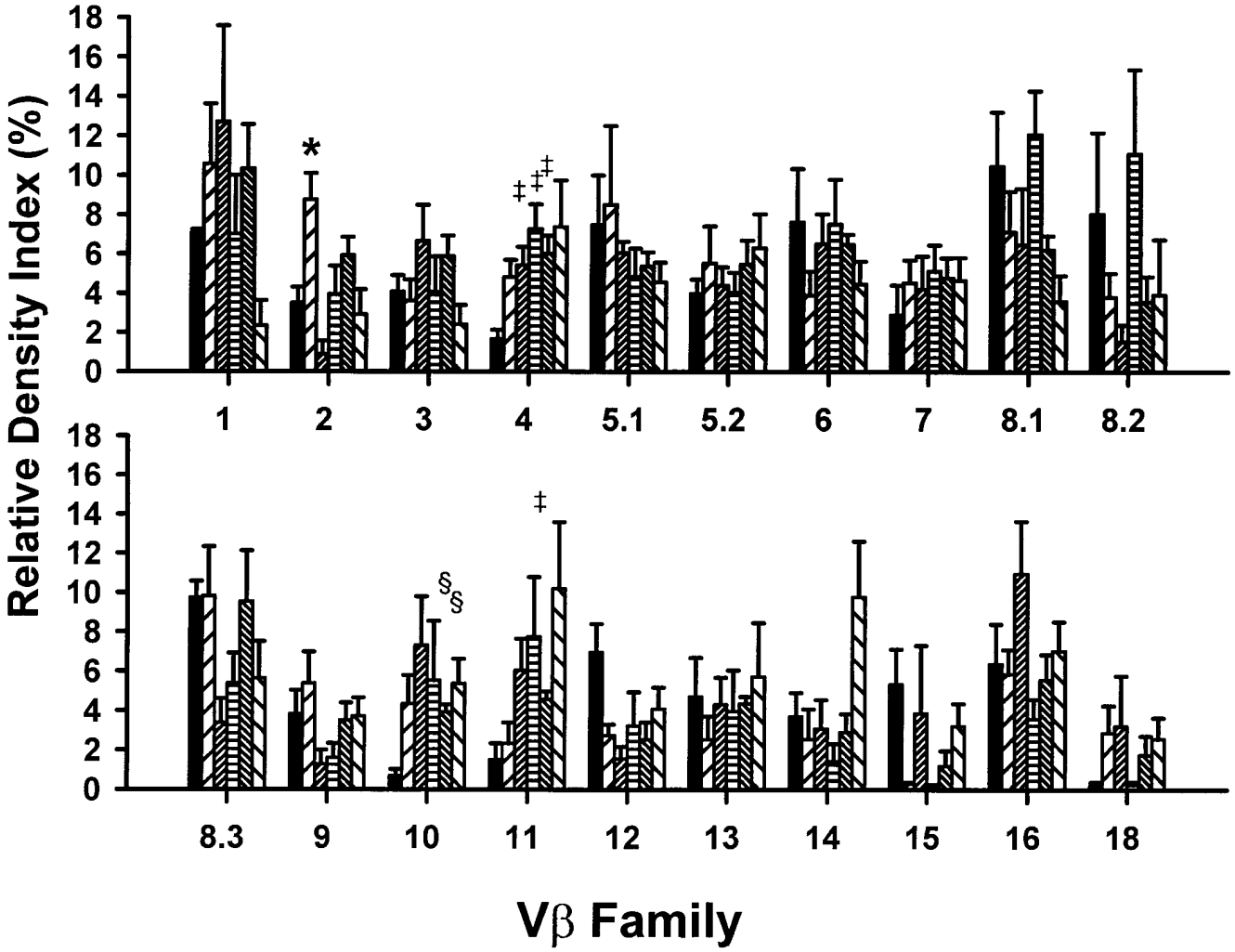

Figure 4. Analysis of the Vβ usage during infection with Hc. Total RNA was extracted from lungs of mice infected with Hc for 3 (striped bar, upward diagonal), 7 (narrow striped bar, upward diagonal), 10 (horizontal striped bar), 14 (narrow striped bar, downward diagonal), and 21 (striped bar, downward diagonal) d, or from uninfected controls (solid bar). RNA was reverse transcribed and each Vβ family was amplified by PCR and visualized by Southern blot. For every mouse, the Rdi was computed. Each bar represents the mean±SEM of six mice. The Rdi at every time point was compared with the respective Rdi in the control. Statistically significant differences are denoted by the symbols: $^{*}P < 0.02$; $^{\ddagger}P < 0.01$; $^{\S}P < 0.04$.

lyzed using confidence intervals, similar differences were noted.

The variations in the quantity of mRNA may be the result of either increased transcription or an increase in the number of a given cell population. To determine if the elevations in the relative density index actually indicated an expansion in Vβ cell populations, we analyzed surface expression of selected Vβ families using flow cytometry (Fig. 5). In lungs from mice infected for 10 d, 10.1±0.7% of T cells were Vβ4^{+}, whereas in the control mice this cell population comprised only 3.5±0.6% of T cells ($P < 0.01$). No significant differences were observed for Vβ10, Vβ11, or Vβ5 (Fig. 5). Thus, the differences in Rdi indicate a true accumulation of Vβ4^{+} cells.

Sequence analysis of Vβ4 PCR products. Our observations indicated that the Vβ4^{+} subset of T cells is significantly overrepresented on days 7, 10, and 14 after infection, a time period that coincides to the peak of cell infiltration and cytokine production in the lung (6). Consequently, we analyzed the Vβ4 repertoire in further detail. We isolated Vβ4 PCR products from mice at days 7 ($n = 5$), 10 ($n = 3$), and 14 ($n = 3$) after infection, cloned them into plasmid, and transformed them into *E. coli.* 10–20 random colonies were picked for sequence determination. Vβ4 PCR products from three uninfected mice were used as controls. The sequences and the frequency analysis of the CDR3 are depicted in Table I. The Vβ4^{+} repertoire was found to be heterogeneous, as seen in mice A and B. On the other hand, sequences from control mouse C distributed into three clonotypes.

On day 7 after infection, there was evidence of oligoclonality in sequences of mice A, D, and E (Table I), as 40–60% of the Vβ4^{+} sequences belonged to a specific clonotype. The Vβ4^{+} repertoire of mice C and B did not show oligoclonality. As the infection evolved, the observed oligoclonality became less apparent, as most of the sequences seen on days 10 to 14 after infection were more diverse.

Inspection of the deduced amino acid sequences at the CDR3 level showed several instances of common motifs among infected mice: on day 7, postinfection mice A and D ex-

*Table I. Deduced Amino Acid Sequence at the Vβ4 CDR3 Domain from Control and Infected Mice**

Mouse	Vβ4	CDR3	Jβ	Cβ	Frequency	Dβ Family	Jβ
Control A	CASSQ	EGQ	NSDYTFGSGTRLLVI	EDLRNVTP	3/11	1	1.2
	CASSQ	DPGT	RNERLFFGHGTKLSVL	EDLRNVTP	1/11	1	1.4
	CASSQ	EDR	NTGQLYFGEGSKLTVL	EDLRNVTP	1/11	1	2.2
	CASSQ	DPA	SQNTLYFGAGTRLSVL	EDLRNVTP	1/11	2	2.4
	CASS	RDR	YEQYFGPGTRLTVL	EDLRNVTP	1/11	1	2.6
	CASS	QDWG	SYEQYFGPGTRLTVL	EDLRNVTP	3/11	2	2.6
	CASS	HLWGGE	YEQYFGPGTRLTVL	EDLRNVTP	1/11	2	2.6
Control B	CASSQ	RDK	NTEVFFGKGTRLTVV	EDLRNVTP	1/13	1	1.1
	CASSQ	DDREG	SDYTFGSGTRLLVI	EDLRNVTP	1/13	1	1.2
	CASSQ	DPGQG	NERLFFGHGTKLSVL	EDLRNVTP	1/13	1	1.4
	CAS	RD	TNERLFFGHGTKLSVL	EDLRNVTP	1/13	1	1.4
	CASS	HQGLG	QAPLFGEGTRLSVL	EDLRNVTP	1/13	2	1.5
	CASSQ	DPGQGS	QDTQYFGPGTRLLVL	EDLRNVTP	1/13	1	2.5
	CASSQ	DLG	EDTQYFGPGTRLLVL	EDLRNVTP	2/13	2	2.5
	CASSQ	VGG	SYEQYFGPGTRLTVL	EDLRNVTP	1/13	?	2.6
	CASS	RGTGA	YEQYFGPGTRLTVL	EDLRNVTP	1/13	2	2.6
	CASS	PRLGV	SYEQYFGPGTRLTVL	EDLRNVTP	1/13	2	2.6
	CASSQ	ERGGS	SYEQYFGPGTRLTVL	EDLRNVTP	2/13	?	2.6
Control C	CASSQ	GGLG	NTGQLYFGEGSKLTVL	EDLRNVTP	5/10	2	2.2
	CASS	QTD	SQNTLYFGAGTRLSVL	EDLRNVTP	3/10	1	2.4
	CAS	SIMDRG	NQDTQYFGPGTRLLVL	EDLRNVTP	2/10	1	2.5
Day 7A	CASSQ	T	TNSDYTFGSGTRLLVL	EDLRNVTP	1/11	?	1.2
	CASSQ	*EARGR*‡	*SDY*TFGSGTRLLVI	EDLRNVTP	1/11	?	1.2
	CASS	QQG	YNSPLYFAAGTRLTVT	EDLRNVTP	4/11	1	1.6
	CASSQ	DGTGGA	EQFFGPGTRLTVL	EDLRNVTP	5/11	2	2.1
Day 7 B	CASSQ	DITGGF	SDYTFGSGTRLLVI	EDLRNVTP	1/12	1	1.2
	CASS	*QGT*§	*ISN*ERLFFGHGTKLSVL	EDLRNVTP	4/12	1	1.4
	CASSQ	DRG	YAEQFFGPGTRLTVL	EDLRNVTP	2/12	1	2.1
	CASSQ	DG	SQNTLYFGAGTRLSVL	EDLRNVTP	3/12	?	2.4
	CASSQ	DLGGPL	EQYFGPGTRLTVL	EDLRNVTP	1/12	2	2.6
	CASSQ	DPGLG	AYEQYFGPGTRLTVL	EDLRNVTP	1/12	2	2.6
Day 7 C	CASS	QTGTG	NTEVFFGKGTRLTVV	EDLRNVTP	1/16	1	1.1
	CASS	LTGDG	SDYTFGSGTRLLVI	EDLRNVTP	1/16	?	1.2
	CASS	HTN	SGNTLYFGEGSRLIVV	EDLRNVTP	2/16	?	1.3
	CASSQ	QG	AGNTLYFGEGSRLIVV	EDLRNVTP	1/16	1	1.3
	CASS*Q*	*GT*§	*ISN*ERLFFGHGTKLSVL	EDLRNVTP	2/16	1	1.4
	CASS	QGT	DQAPLFGEGTRLSVL	EDLRNVTP	2/16	1	1.5
	CASS	QDI	NNQAPLFGEGTRLSVL	EDLRNVTP	1/16	1	1.5
	CASSQ	DTV	NNQAPLFGEGTRLSVL	EDLRNVTP	1/16	?	1.5
	CASSQ	EGN	QNTLYFGAGTRLSVL	EDLRNVTP	1/16	?	2.4
	CASS	R	EDTQYFGPGTRLLVL	EDLRNVTP	1/16	?	2.5
	CASSQ	EGDL	QDTQYFGPGTRLLVL	EDLRNVTP	1/16	?	2.5
	CASSQ	D	SYEQYFGPGTRLTVL	EDLRNVTP	1/16	1	2.6
	CASS	QGQGI	YEQYFGPGTRLTVL	EDLRNVTP	1/16	1	2.6
Day 7 D	CASSQ	EARGR‡	SDYTFGSGTRLLVI	EDLRNVTP	8/14	?	1.2
	CASSQ	RSG	DAEQFFGPGTRLTVL	EDLRNVTP	6/14	1	2.1

(Continued)

Table I (Continued)

Mouse	Vβ4	CDR3	Jβ	Cβ	Frequency	Dβ Family	Jβ
Day 7 E	CASS	PGGE	DTEVFFGKGTRLTVV	EDLRNVTP	4/12	?	1.1
	CASS*Q*	*GT*[§]	*ISN*ERLFFGHGTKLSVL	EDLRNVTP	5/12	1	1.4
	CASSQ	EWRGRLQ	APLFGEGTRLSVL	EDLRNVTP	2/12	?	1.5
	CASSQ	DGTGGV	EQYFGPGTRLTVL	EDLRNVTP	1/12	2	2.6
Day 10 A	CASS	LTGA	NTEVFFGKGTRLTVV	EDLRNVTP	1/12	1	1.1
	CASSQ	EG	ANTEVFFGKGTRLTVV	EDLRNVTP	1/12	?	1.1
	CASSQ	EGQ	ANTEVFFGKGTRLTVV	EDLRNVTP	1/12	1	1.1
	CASSQ	DGGQGG	SDYTFGSGTRLLVI	EDLRNVTP	2/12	1	1.2
	CASSQ	Q	IPTKDYFSGHGTKLSVL	EDLRNVTP	1/12	?	1.4
	CASS	HTGG	NERLFFGHGTKLSVL	EDLRNVTP	1/12	1	1.4
	CASS**Q**	**G**[¶]	**DYAE**QFFGPGTRLTVL	EDLRNVTP	1/12	?	2.1
	CASSQ	**QG**[¶]	**NYAE**QFFGPGTRLTVL	EDLRNVTP	1/12	1	2.1
	CASSQ	DGGL	NAEQFFGPGTRLTVL	EDLRNVTP	1/12	2	2.1
	CASSQ	EKTR	YFGPGTRLTVL	EDLRNVTP	1/12	?	2.6
	CASSQ	DWTGGD	EQYFGPGTRLTVL	EDLRNVTP	1/12	1	2.6
Day 10 B	CASS	QTR	NSDYTFGSGTRLLVI	EDLRNVTP	1/15	2	1.2
	CASSQ	DKN	SGNTLYFGEGSRLIVV	EDLRNVTP	1/15	?	1.3
	CASSQ	DA	FSNERLFFGHGTKLSVL	EDLRNVTP	1/15	?	1.4
	CASS	LDRNQ	APLFGEGTRLSVL	EDLRNVTP	1/15	?	1.5
	CASSQ	EG	DSYNSPYFAAGTRLTVT	EDLRNVTP	1/15	?	1.6
	CASSQ	QS	NYAEQFFGPGTRLTVL	EDLRNVTP	1/15	2	2.1
	CASS	Q**QG**[¶]	**NYAE**QFFGPGTRLTVL	EDLRNVTP	1/15	?	2.1
	CASSQ	GTGAVS	AETLYFGSGTRLTVL	EDLRNVTP	2/15	1	2.3
	CASSQ	EGTS	SQNTSYFGAGTRLSVL	EDLRNVTP	3/15	1	2.4
	CASSQ	DGGL	NQDTQYFGPGTRLLVL	EDLRNVTP	1/15	2	2.5
	CASSQ	DTGGP	YEQYFGPGTRLTVL	EDLRNVTP	1/15	2	2.6
	CASSQ	EWGAQ	YEQYFGPGTRLTVL	EDLRNVTP	1/15	?	2.6
Day 10 C	CASS	DRD	NYAEQFFGPGTRLTVL	EDLRNVTP	2/10	?	2.1
	CASSQ	ERDS	YAEQFFGPGTRLTVL	EDLRNVTP	1/10	1	2.1
	CASS	PGG	ENTLYFGAGTRLSVL	EDLRNVTP	1/10	?	2.4
	LCQQ	RD	SQNTLYFGAGTRLSVL	EDLRNVTP	1/10	?	2.4
	CASSQ	DWGV	QNTLYFGAGTRLSVL	EDLRNVTP	1/10	2	2.4
	CASSQ	DWG	QDTQYFGPGTRLLVL	EDLRNVTP	1/10	2	2.5
	CAS	RRLGG	HQDTQYFGPGTRLLVL	EDLRNVTP	1/10	?	2.5
	CASS	PGGV	EQYFGPGTRLTVL	EDLRNVTP	1/10	?	2.6
	CASSQ	DLGR	YEQYFGPGTRLTVL	EDLRNVTP	1/10	?	2.6
Day 14 A	CASSQ	PG	PNTEVFFGKGTRLTVV	EDLRNVTP	1/10	?	1.1
	CASSQ	GQ	FSNERLFFGHGTKLSVL	EDLRNVTP	1/10	1	1.4
	CASSQ	ERGRV	AEQFFGPGTRLTVL	EDLRNVTP	2/10	?	2.1
	CASSQ	DPGG	NYAEQFFGPGTRLTVL	EDLRNVTP	2/10	?	2.1
	CASSQ	DSGG	YTGQLYFGEGSKLTVL	EDLRNVTP	1/10	?	2.2
	CASSQ	GTGGD	AETLYFGSGTRLTVL	EDLRNVTP	1/10	?	2.3
	CASSQ	EVGR	DQDTQYFGPGTRLLAL	EDLRNVTP	1/10	?	2.5
	CASSQ	ETLWG	DQDTQYFGPGTRLLVL	EDLRNVTP	1/10	?	2.5
	CASSQ	ELGGL	EQYFGPGTRLTVL	EDLRNVTP	1/10	2	2.6

(Continued)

Table I. (Continued)

Mouse	Vβ4	CDR3	Jβ	Cβ	Frequency	Dβ Family	Jβ Family
Day 14 B	CASSQ	EAG	ANTEVFFGKGTRLTVV	EDLRNVTP	1/10	?	1.1
	CASSQ	**QG**¶	**NYAE**QFFGPGTRLTVL	EDLRNVTP	2/10	1	2.1
	CASS	P**QG**¶	**NYAE**QFFGPGTRLTVL	EDLRNVTP	1/10	?	2.1
	CASS	QSGG	SQNTLYFGAGTRLSVL	EDLRNVTP	1/10	2	2.4
	CASS	PGLE	GQNTLYFGAGTRLSVL	EDLRNVTP	1/10	2	2.4
	CASSQ	EGTT	SQNTLYFGAGTRLSVL	EDLRNVTP	1/10	1	2.4
	CASS	PGQ	QDTQYFGPGTRLLVL	EDLRNVTP	1/10	1	2.5
	CASSQ	EVG	SSYEQYFGPGTRLTVL	EDLRNVTP	2/10	?	2.6
Day 14 C	CASSQ	DR	DTEVFFGKGTRLTVV	EDLRNVTP	1/10	?	1.1
	CASS	SGT	TNSDYTFGSGTRLLVI	EDLRNVTP	1/10	1	1.2
	CASSQ	DPGG	HSDYTFGSGTRLLVI	EDLRNVTP	1/10	1	1.2
	CASS	RTGRI	ERLFFGHGTKLSVL	EDLRNVTP	1/10	1	1.4
	CASSQ	GT	VSNERLFFGHGTKLSVL	EDLRNVTP	1/10	?	1.4
	CASS**Q**	**G**¶	**DYAE**QFFGPGTRLTVL	EDLRNVTP	2/10	?	2.1
	CASS	PGLG	ENTLYFGAGTRLSVL	EDLRNVTP	1/10	2	2.4
	CASS	QGRGL	GQNTLYFGAGTRLSVL	EDLRNVTP	1/10	?	2.4
	CASSQ	DGV	DTQYFGPGTRLLVL	EDLRNVTP	1/10	?	2.5

*Vβ4 PCR products from control mice or 7, 10, and 14 d after infection were reamplified using Vβ4 sense primer and the Cβ3 nested antisense primer. DNA was gel purified and cloned into PCR2.1® vector. 10–20 clones per mouse were sequenced, and deduced amino acid sequences are shown in the table. Sequences were submitted to GenBank. Accession numbers are AF041867 to AF041974. When sequences were found in more than one clone, only one was submitted. ‡Sequences common to mouse A and D at day 7 are underlined. §Sequences common to mouse B, C, and E at day 7 are shown in italics. ¶The common motifs Q, G,(N or D),YAE at days 10 and 14 are shown in boldface.

pressed the sequence QEARGR followed by the Jβ1.2 element; mice B, C, and E contained the sequence QGTI followed by the Jβ1.4 element. On days 10 and 14 the motif (q)QG(N or D)YAE followed by the Jβ2.1 element was observed in six independent clones.

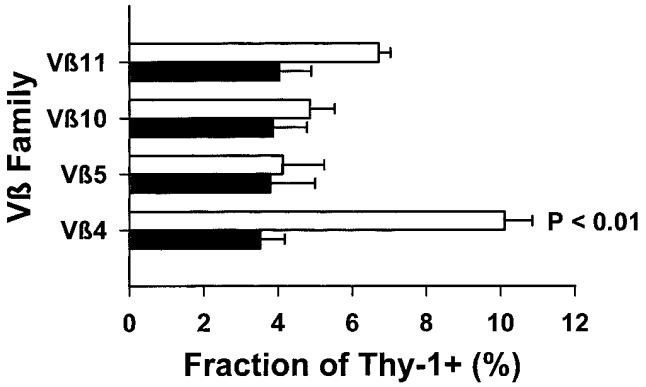

Figure 5. Analysis of selected Vβ families by flow cytometry. Mononuclear cells were isolated from lungs of mice infected for 10 d with Hc (solid bar) or from uninfected controls (white bar). Cells were stained at 4°C with biotinylated mAb against TCR Vβ chains 4, 10, 11, and 5, and with fluorescein Thy-1 mAb, or with isotype-matched irrelevant control mAb to determine the background staining. Cells were washed and then incubated with phycoerythrin-streptavidin. The number of cells staining positive for each Vβ chain minus background was divided by the total number of Thy-11 cells minus the background and expressed as a percentage. Each bar is the mean±SEM of six mice. Statistically significant differences are shown in the graph.

We also analyzed the Jβ and Dβ use of the Vβ4 sequences. There was a pronounced bias in the Jβ use (Table II). The Jβ2.1 sequence constituted 19% of independent sequences on day 7 of postinfection, 24% on day 10, and 22% on day 14. In uninfected animals none of the 30 Vβ4 TCR sequences contained the Jβ2.1 element.

*Table II. Jβ Element Use in Vβ4 TCR among Infected and Control Mice**

Jβ Element	Control	Infected Day 7	Infected Day 10	Infected Day 14
1.1	3%	7%	8%	9%
1.2	11%	19%	8%	6%
1.3	0%	4%	3%	0%
1.4	18%	17%	8%	9%
1.5	3%	10%	0%	0%
1.6	0%	6%	3%	0%
2.1	0%	**19%**‡	**24%**‡	**22%**‡
2.2	13%	0%	0%	3%
2.3	0%	0%	5%	9%
2.4	13%	6%	16%	19%
2.5	11%	3%	8%	9%
2.6	29%	9%	16%	13%

*The sequences of the Vβ4 TCR chains of uninfected mice and days 7, 10, and 14 after infection were pooled, and the relative frequency of each Jβ element was determined and expressed as a percent of the total. ‡Frequency of the Jβ2.1 element in infected mice is highlighted.

Effects of Vβ4 depletion in resistance against Hc. Next, we sought to determine the relevance of the Vβ4$^+$ subpopulation of T cells to host defenses as this family was prominent during the critical period of infection. To accomplish this, mice were depleted selectively of this population in vivo using anti-Vβ4 mAb. As a control, separate groups of mice were given rat IgG. After 1 wk, mice were challenged with 2.5×10^6 Hc yeasts intranasally. To ascertain if the administration of anti-Vβ4 eliminated this cell population, RNA was prepared from the lungs of treated mice or from rat IgG–treated, infected controls. The RNA was reverse transcribed, and the cDNA was analyzed by PCR and Southern blot using Vβ4, Vβ7, or Cβ primers. As seen in Fig. 6 *A*, treatment with anti-Vβ4 nearly abrogated the mRNA for this cell population.

The effect of Vβ4 depletion on the course of infection was assessed by quantitative organ cultures. Mice were killed at days 7, 14, and 21 after infection and the fungal burden was compared to rat IgG-treated controls. No differences in CFU were observed on day 7. However, on days 14 and 21 of infection, recovery of Hc from lungs of mice depleted of Vβ4$^+$ T cells significantly exceeded ($P < 0.01$) that of infected controls,

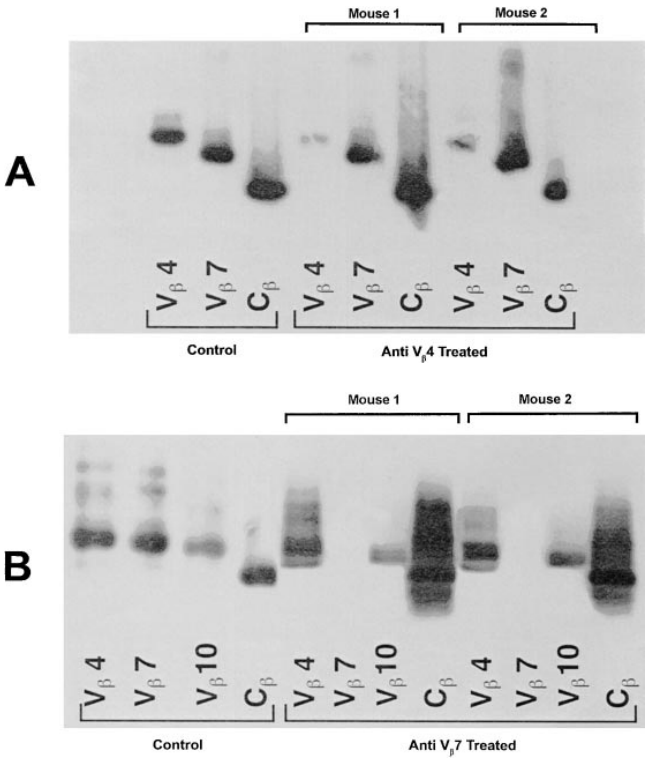

Figure 6. Southern blot assessment of in vivo depletion of Vβ families using mAb. (*A*) Groups of mice were injected intraperitoneally with 300 μg of anti-Vβ4 or rat IgG as control on days −7, −3, and 0 of infection. Mice were infected intranasally with 2.5×10^6 Hc yeasts. 1 wk later mice were killed and total RNA was extracted from the lungs, and cDNA synthesized. PCR was performed using Vβ4, Vβ7, and Cβ primers, and the DNA electrophoresed in 1% agarose. Amplified DNA was blotted on nylon membranes and probed with a digoxigenin-labeled Cβ probe. One control and two treated mice depicted in the figure. (*B*) Groups of mice were injected with the anti-Vβ7 mAb or rat IgG as described in *A*. PCR analysis was performed with Vβ4, Vβ7, Vβ10, and Cβ primers. One control and two treated mice depicted in the figure.

(Fig. 7 *A*). The results in livers and spleens were less consistent in experiment number 1. Although the fungal burden was higher in mice depleted of Vβ4$^+$ T cells as compared to infected controls, the mice lacking Vβ4$^+$ were capable of clearing the infection albeit at a less accelerated rate than controls. However, the impairment of host resistance was not associated with a higher mortality since 100% of controls and Vβ4$^+$-depleted animals survived for 40 d after infection.

We subsequently tested the hypothesis that the observed delay in clearance of infection was the result of either a quantitative reduction in the number of T cells or a qualitative, distinct contribution of the Vβ4$^+$ T cell subpopulation. To test this postulate, we chose the Vβ7$^+$ T cell subpopulation for a control study. The relative density index of Vβ7 was comparable to that of Vβ4 during the period of 7 to 14 d after infection (Fig. 4). In a parallel experiment, we injected mice with anti-Vβ7 mAb or rat IgG as control and infected them intranasally with 2.5×10^6 Hc. On day 7 of infection, we tested the depleting activity of the anti-Vβ7 by reverse transcriptase-PCR and Southern blot analysis. The mAb was as effective and as specific as anti-Vβ4 (Fig. 6 *B*).

We then examined the impact of Vβ7$^+$ T cell depletion in the course of infection with Hc. In two experiments, depletion of Vβ7$^+$ T cells did not significantly ($P > 0.05$) alter CFU recovery in lungs, livers, or spleens when compared to controls (Fig. 7 *B*). These results indicate that the depletion of Vβ4$^+$ cells was associated with a selective impairment in host resistance to Hc.

Levels of IFN-γ in lungs of mice depleted of Vβ4$^+$ T cell subpopulation. The lymphokine IFN-γ is a product of Th1 and natural killer cells and is pivotal in host resistance against Hc infection in C57BL/6 mice (22, 23). We tested the hypothesis that the delayed clearance of Hc observed in Vβ4-depleted mice was associated with impaired production of IFN-γ in the lungs of mice. We quantified the lymphokine in homogenates of lungs from animals depleted of Vβ4$^+$ cells and controls at days 7, 14, and 21 after infection (Fig. 8). No significant differences ($P > 0.05$) were detected between the groups at each time point. Thus, the effect of Vβ4 depletion on the course of infection cannot be attributed to a perceptible impairment in IFN-γ generation in the lungs of infected mice.

Discussion

The extraordinary diversity of the TCR repertoire is generated by a specialized mechanism of recombination during the differentiation of T cells. The repertoire is molded by a variety of influences including the MHC antigens expressed on antigen-presenting cells, intrathymic positive and negative selection, peripheral tolerance, the presence of endogenous superantigens, and environmental stimuli (15, 24). Microbial antigens, either in the form of replicating organisms or as inert protein molecules, are one of the common environmental exposures known to alter the host's TCR repertoire, and engagement of the cognate determinants may prompt expansion or deletion of particular TCR families (25, 26). Thus, the TCR repertoire is highly dynamic and has evolved to confront a diverse array of antigenic challenges.

The generation of T cell–mediated immunity is a critical determinant of host control of infection with Hc. Both CD4$^+$ and CD8$^+$ T cells participate in the elimination of the organism from visceral organs (7, 9). Because T cells are arranged as

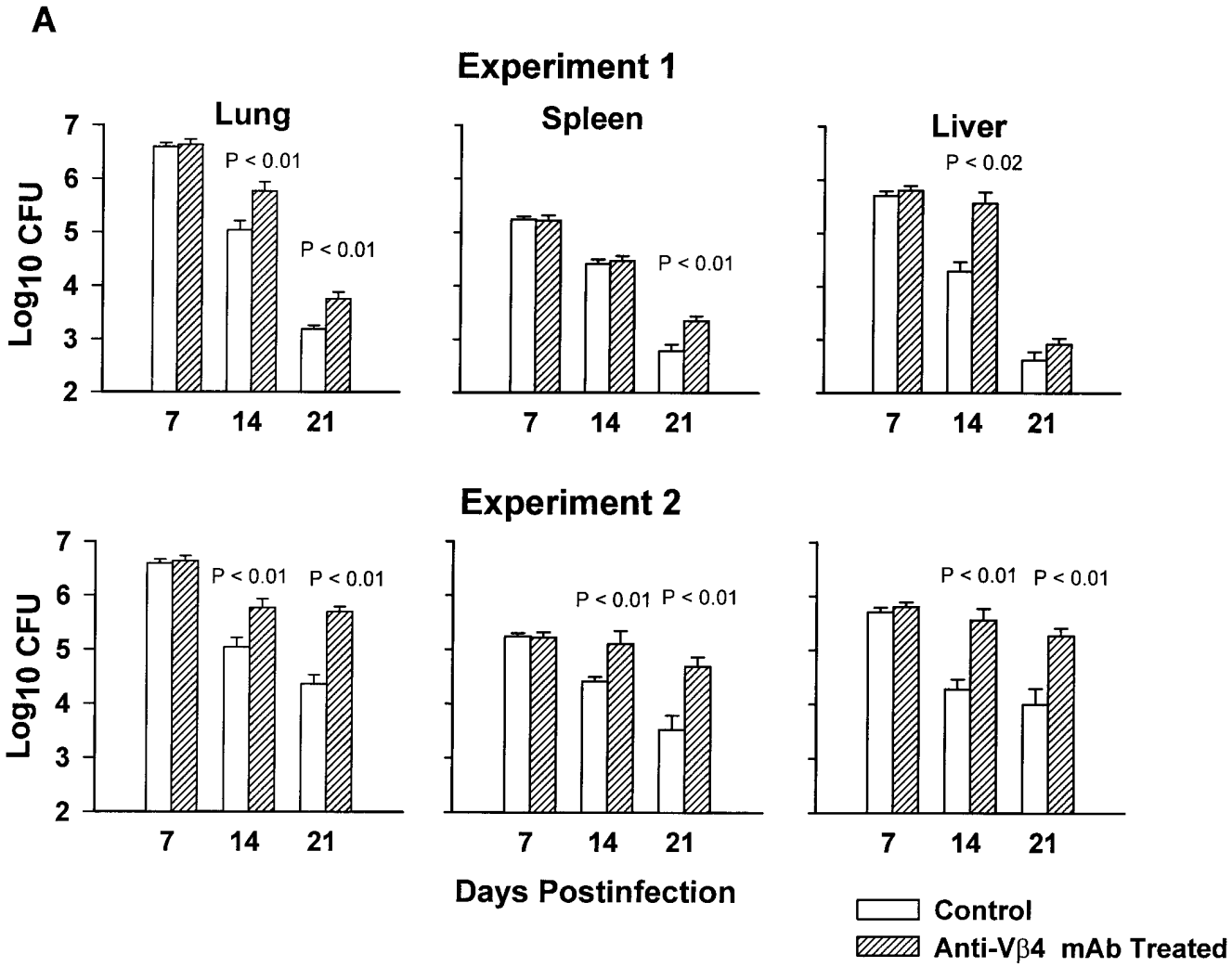

Figure 7. Depletion of Vβ4, but not Vβ7 cells, alters clearance of Hc. (*A*) Groups of mice were given intraperitoneal injections of 300 μg of anti-Vβ4 or rat IgG as a control on days −7, −3, and 0 of infection. Mice were infected with 2.5×10^6 yeasts intranasally. When the experiments were extended beyond 1 wk, mice received 300 μg of anti-Vβ4 or rat IgG twice a week. Mice were killed on days 7, 14, and 21 after infection, and organs homogenized in 10 ml of HBSS. Dilutions were plated in blood agar plates and CFU quantified. Results are expressed as Log10 CFU/organ. Each bar is the mean±SEM of six mice per time point and per group. Significant differences are noted by the *P* value. (*B*) Groups of mice were administered 300 μg of either anti-Vβ7 or rat IgG on days −7, −3, and 0. Mice were infected and CFU were quantified as in *A*.

a series of clones, definition of the TCR repertoire in Hc infection may lead to basic insights into the nature of the T cell response and the pathogenesis of infection. Hence, we examined the Vβ TCR repertoire in lungs of C57BL/6 mice after intranasal inoculation with yeasts. We chose the lung because it is the portal of entry for this fungus, and we used a sublethal challenge because most human exposures do not result in disease that requires medical attention.

The approaches to the study of the TCR repertoire have largely been conducted on monoclonal populations of T cells using either reverse transcriptase-PCR–based techniques or flow cytometry (20, 27, 28). Examination of monoclonal populations of T cells usually provides unambiguous information concerning expression of Vβ at the single cell level. The drawback of in vitro propagated clones is that the diversity of TCR expression may be lost because the clonal analysis is restricted to those that survive the expansion process. This information may not be entirely germane for an infectious disease, in which host tissues are confronted with an actively replicating pathogen that may contain hundreds to thousands of putative antigens. Ex vivo analysis of Vβ expression used herein should yield a more panoramic view of the complexity of TCR usage during the course of Hc infection. Moreover, we centered our efforts on the Vβ chain because of its prominent role in epitope binding (29, 30, 31).

The time points selected for analysis spanned the early phase of infection (day 3), the peak (days 7 and 10), and the resolving phases (days 14 and 21). In the lungs of C57BL/6 mice infected with Hc, a flux in the Vβ repertoire was apparent. During days 7, 10, and 14 of infection, the $V\beta4^+$ subset of T cells was substantially expanded and then subsided. This expansion was coincident with peak of infection and the initiation of clearance. Hence, $V\beta4^+$ T cells were significantly elevated during a critical period of infection. The encounter of T cells with foreign antigenic determinants is a major factor in the shaping of the Vβ repertoire in adult mammals. Hence, the

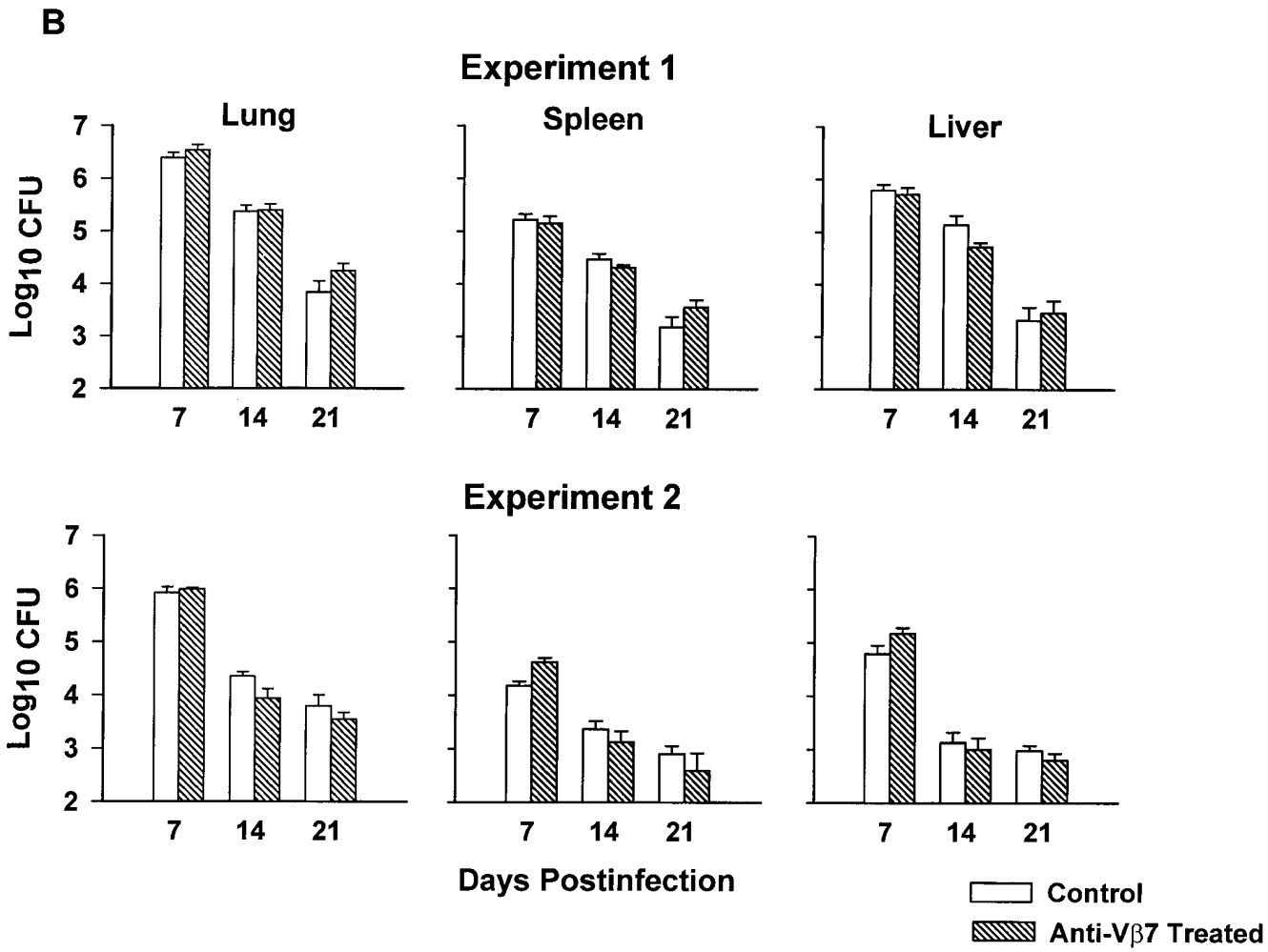

Figure 7 (Continued)

epitopes recognized by T cells are a prominent driving force in the expansion of clonotypes. Because we detected expansion of several Vβ during the course of infection, the findings strongly suggest that different epitopes are generated by antigen-presenting cells. These epitopes bound to MHC are principally responsible for the increase in the Vβ families.

This expansion of the Vβ4$^+$ subpopulation could be explained by the presence of a superantigen within viable Hc yeast cells. However, the oligoclonality detected on day 7 is not consistent with this postulate. Superantigens most often induce a CDR3-independent, polyclonal expansion in the repertoire. Moreover, superantigens usually cause expansion of more than one Vβ family, and the magnitude is much greater (32). Alternatively, the bias towards Vβ4-bearing T cells may be driven by many antigenic determinants that increase the number of cells in this Vβ subset. The sequencing data does not support this contention. In several instances, the same CDR3 sequence was independently found in more than one mouse (Table I). This finding of limited heterogeneity in TCR sequences has been referred to as a "public" TCR sequence, and has been observed most often after immunization with a well defined, synthetic peptide antigen (27, 33, 34). It is considered to be the result of the interaction of a unique antigenic peptide presented by the MHC with a highly restricted subset of Vβ cells. Thus, the oligoclonal character of the Vβ4 sequences on day 7 is most consistent with the presence of a restricted set of epitopes that increase Vβ4$^+$ cells.

The TCR oligoclonality observed on day 7 was not detected on days 10 or 14. This phenomenon of early oligoclonality that progresses to a less restricted response has been observed in models of autoimmunity (35). One explanation is that as the infection proceeds, there is recruitment and influx of many Vβ families including Vβ4$^+$ cells to the infection site. This nonspecific emigration of T cells at the later stages of infection may attenuate the initial oligoclonality or frustrate attempts to identify it.

Sequence analysis of the Vβ4 CDR3 from control mice revealed polyclonality in two of three mice. Vβ4 sequences from mouse C were restricted into three patterns. This finding may be explained by the paucity of this family of T cells in the lungs of control mice. In uninfected mice, the number of T cells recoverable from lungs is $< 10^5$, and the Vβ4$^+$ T cells constitute $\sim$ 3.5% of the total. Consequently, quantities of mRNA are low, and it may be more difficult to isolate independent cDNA clones. In this regard, it was necessary to generate large numbers of cDNA clones and perform a filter hybridization step from the lungs of normal mice to isolate Vβ4 positive clones. Conversely, in lungs of infected mice, there is a substantial elevation in the numbers of T cells ($\sim 10^7$), and the Vβ4 family constitutes a higher proportion ($\sim$ 10%). Thus, amounts of

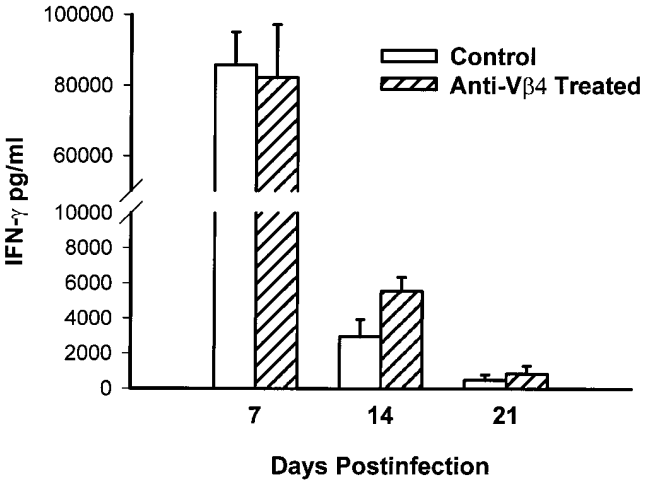

Figure 8. IFN-γ levels in lungs of Vβ4-depleted mice. Groups of mice were injected with anti-Vβ4 or with rat IgG as described in Fig. 6. After intranasal inoculation with Hc, mice were killed at weeks 1, 2, and 3 after infection. Lungs were homogenized in 10 ml of HBSS and IFN-γ levels were determined by antigen-capture ELISA. Each bar represents the mean±SEM of six mice per time point. No statistical difference was found when depleted mice were compared with controls.

mRNA are more abundant, and independent cDNA clones are more readily generated.

On days 7, 10, and 14 of infection, there was a consistent bias in the use of the Jβ 2.1 element in infected mice when compared to controls. The Jβ 2.1 element encodes the amino acid residues at the carboxy terminus of the CDR3 region with the motif: QG(N or E)YAE (Table I). This pattern was found with increased frequency in the TCR of infected animals and was not detected in any of the 30 cDNA clones from normal mice. Because the Jβ portion of the TCR binds to the peptide epitope attached to the MHC molecule, this expansion of the $V\beta4^+$, $J\beta2.1^+$ population suggests that during days 7 to 14, a limited set of antigenic determinants are recognized by this T cell family. Studies are in progress to define the amino acid sequence of the Hc peptide epitope that binds to this TCR family.

It seems surprising that exposure to a replicating microbe such as the yeast phase of Hc would elicit a bias towards discrete Vβ families and CDR3 motifs. Nevertheless, others have detected oligoclonal TCR responses against complex infectious agents including viruses (36, 37) and *Leishmania major*. Our data extend the observations that infection with a eukaryotic pathogen can induce a skewing of the TCR repertoire. Thus, despite the vast complexity of the genome of pathogenic microbes, especially eukaryotes, a pattern emerges whereby certain antigens are preferentially processed and recognized by a particular family of T cells.

Reiner et al. (38) demonstrated that infection with *L. major* resulted in an expansion of $V\beta4^+$ T cells in both resistant and susceptible strains of mice (C57BL/6 and BALB/c, respectively). In this model, $V\beta4^+$ cells can express either Th1 or Th2 activity depending on the genetic background of the mouse (38, 39). It is intriguing to speculate that infection with eukaryotic intracellular pathogens may augment growth of this family. However, this possibility awaits additional analyses of TCR repertoire with other intracellular eukaryotic pathogens. Moreover, the likelihood that $V\beta4^+$ cells derived from *L. major*–infected animals recognize similar epitopes as do those from *H. capsulatum*–infected mice is unlikely, as the CDR3 sequences of *L. major*–specific $V\beta4^+$ cells differ from those identified in our study (38).

After we established that infection with Hc elicited the expansion of the $V\beta4^+$ subpopulation of T cells, it was germane to determine the relevance of this subset in host resistance against the fungus. To examine the in vivo importance of $V\beta4^+$ cells to host defense, these cells were eliminated by injection with mAb. One important caveat in interpreting these studies is that this mAb eliminates all $V\beta4^+$ cells, irrespective of the CDR3 region or Jβ and Dβ usage, and irrespective of the functional phenotype. This lack of specificity is unavoidable as this mAb eliminates all $V\beta4^+$ cells. Nonetheless, depletion of $V\beta4^+$ cells was accompanied by a significant delay in the clearance of infection at week 2 and 3 after infection. Although elimination of this T cell subset impaired clearance, mice were still capable of resolving the infection. In contrast, depletion of $V\beta4^+$ cells did not alter the fungal burden at week 1, thus indicating that this cell population is not critical for resolution during the early phase of infection.

Elimination of Hc is associated with a Th1 response in lungs of C57BL/6 mice (22). The loss of $V\beta4^+$ cells and the attendant impairment of clearance signifies that this population contributes to the generation of a Th1 response. In a similar vein, *L. major*–reactive $V\beta4^+$ cells can direct the development of a Th1 or Th2 response in resistant or susceptible mice (38, 39). Abolition of $V\beta4^+$ $V\beta8^+$ $CD4^+$ cells from BALB/c mice shifts the susceptible phenotype to a resistant one (39). Therefore, a small subpopulation of T cells can exert pronounced effects on the type of immune response generated to a pathogenic microbe.

It was possible that the observed effect of depletion of $V\beta4^+$ cells on course of infection could be explained by a quantitative 10% reduction in the number of T cells rather than a distinct quality of these cells. To test this possibility, we selected the Vβ7 family whose percentage was nearly identical to that of Vβ4 in infected animals. Depletion of this Vβ family did not modulate clearance. These results indicate that elimination of any Vβ family that constitutes $\sim$ 10% of the total T cell population does not necessarily modify infection. Thus, the expansion of $V\beta4^+$ cells has an important functional correlate.

It has been suggested that in HIV disease, there is a progressive and random depletion of $CD4^+$ clonotypes altering the TCR repertoire across all Vβ families (40). Susceptibility to microbes ensues when a critical number of pathogen-responsive T cell clones have been lost. Our results point towards the same hypothesis: by specifically disrupting the TCR in a targeted fashion, we can modify the course of the infection in this model of pulmonary histoplasmosis.

IFN-γ is the only cytokine known to be produced by Hc-reactive T cells that is essential in resistance against infection with Hc In C57BL/6 mice (22, 23). We hypothesized that the delayed clearance observed in Vβ4-deficient mice was the result of a defect in the production of IFN-γ in lungs. Cytokine levels were actually higher in treated animals when compared to controls. This result suggests that the effect of $V\beta4^+$ T cells is not caused simply by a global defect in IFN-γ production. Rather, it is possible that elimination of $V\beta4^+$ T cells alters production of IFN-γ within the lung microenvironment. Studies are underway to determine the anatomical distribution of

this cell population, and to analyze the capacity of Vβ4$^+$ cells to generate IFN-γ within the inflamed lung.

An alternative explanation for the effect of Vβ4$^+$ cells on host defenses is that they produce TNF-α, which is known to influence the outcome of primary infection with Hc (41) and can be a product of T cells (42). However, this consideration is most unlikely as we have found that elimination of all TCR α/β–bearing cells from mice does not alter generation of TNF-α from lungs (R. Allendoerfer, G.D. Brunner, and G.S. Deepe, Jr., unpublished observations).

In summary, the Vβ TCR repertoire is biased in the lungs of C57BL/6 mice infected with Hc. Although expression of several families was skewed during the course of infection, the Vβ4 family was overrepresented during the critical juncture of infection. Vβ4$^+$ cells were oligoclonal during the early stages of infection, and these results suggest that an antigen or a group of related antigens propel the expansion and activation of these cells.

Acknowledgments

We thank Todd Greer for technical assistance.

This work was supported by USPHS grants AI-42747 and AI-34361. F.J. Gomez was a Pfizer Post-Doctoral Fellow in Medical Mycology during this work.

References

1. Bullock, W.E. 1993. Interactions between human phagocytic cells and *Histoplasma capsulatum*. *Arch. Med. Res.* 24:219–223.

2. Eisenberg, L.G., P.H. Schlesinger, and W.E. Goldman. 1988. Phagosome-lysosome fusion in P388D1 macrophages infected with *Histoplasma capsulatum*. *J. Leukoc. Biol.* 43:483–491.

3. Newman, S.L., L. Gootee, R. Morris, and W.E. Bullock. 1992. Digestion of *Histoplasma capsulatum* yeasts by human macrophages. *J. Immunol.* 149: 574–580.

4. Williams, D.M., J.R. Graybill, and D.J. Drutz. 1978. *Histoplasma capsulatum* infection in nude mice. *Infect. Immunol.* 21:973–980.

5. Artz, R.P., and W.E. Bullock. 1979. Immunoregulatory responses in experimental disseminated histoplasmosis: depression of T cell-dependent and T-effector responses by activation of splenic suppressor cells. *Infect. Immunol.* 23:893–902.

6. Adamson, D.M., and G.C. Cozad. 1969. Effect of antilymphocyte serum on animals experimentally infected with *Histoplasma capsulatum* or *Cryptococcus neoformans*. *J. Bacteriol.* 100:1271–1276.

7. Gomez, A.M., W.E. Bullock, C.L. Taylor, and G.S. Deepe, Jr. 1988. Role of L3T41 T cells in host defense against *Histoplasma capsulatum*. *Infect. Immunol.* 56:1685–1691.

8. Kauffman, C.A., K.S. Israel, J.W. Smith, A.C. White, J. Schwarz, and G.F. Brooks. 1978. Histoplasmosis in immunosuppressed patients. *Am. J. Med.* 64:923–932.

9. Deepe, G.S., Jr. 1994. Role of CD8$^+$ T cells in host resistance to systemic infection with *Histoplasma capsulatum* in mice. *J. Immunol.* 152:3491–3500.

10. Wheat, L.J., T.G. Slama, and M.L. Zeckel. 1985. Histoplasmosis in the acquired immune deficiency syndrome. *Am. J. Med.* 78:203–210.

11. Wu-Hsieh, B.A., and D.H. Howard. 1987. Inhibition of the intracellular growth of *Histoplasma capsulatum* by recombinant murine γ interferon. *Infect. Immunol.* 55:1014–1016.

12. Newman, S.L., and L. Gootee. 1992. Colony-stimulating factors activate human macrophages to inhibit intracellular growth of *Histoplasma capsulatum* yeasts. *Infect. Immunol.* 60:4593–4597.

13. Newman, S.L., L. Gootee, C. Kidd, G.M. Ciraolo, and R. Morris. 1997. Activation of human macrophage fungistatic activity against *Histoplasma capsulatum* upon adherence to type 1 collagen matrices. *J. Immunol.* 158:1779–1786.

14. Deepe, G.S., Jr. 1994. The immune response to *Histoplasma capsulatum*: unearthing its secrets. *J. Lab. Clin. Med.* 123:201–205.

15. Bevan, M.J., K.A. Hogquist, and S.C. Jameson. 1994. Selecting the T cell receptor repertoire. *Science*. 264:796–797.

16. Marrack, P., and J. Kappler. 1987. The T cell receptor. *Science.* 238: 1073–1079.

17. Matis, L.A. 1990. The molecular basis of T cell specificity. *Annu. Rev. Immunol.* 8:65–82.

18. Davis, M.M. 1990. T cell receptor gene diversity and selection. *Ann. Rev. Biochem.* 59:475–496.

19. Gomez, F.J., A.M. Gomez, and G.S. Deepe, Jr. 1991. Protective efficacy of a 62-kilodalton antigen, HIS-62, from the cell wall and cell membrane of *Histoplasma capsulatum* yeast cells. *Infect. Immunol.* 59:4459–4464.

20. Panzara, M.A., E. Gussoni, L. Steinman, and J.R. Oksenberg. 1992. Analysis of the T cell repertoire using the PCR and specific oligonucleotide primers. *Biotechniques*. 12:728–735.

21. Casanova, J.L., P. Romero, C. Widmann, P. Kourilsky, and J.L. Maryanski. 1991. T cell receptor genes in a series of class I major histocompatibility complex-restricted cytotoxic T lymphocyte clones specific for a *Plasmodium berghei* nonapeptide: implications for T cell allelic exclusion and antigen-specific repertoire. *J. Exp. Med.* 174:1371–1383.

22. Allendoerfer, R., G.P. Boivin, and G.S. Deepe, Jr. 1997. Modulation of immune responses in murine pulmonary histoplasmosis. *J. Infect. Dis.* 175:905–914.

23. Zhou, P., M.C. Sieve, J. Bennett, K.J. Kwon-Chung, R.P. Tewari, R.T. Gazzinelli, A. Sher, and R.A. Seder. 1995. IL-12 prevents mortality in mice infected with *Histoplasma capsulatum* through induction of IFN-γ. *J. Immunol.* 155:785–795.

24. Rozzo, S.J., R.A. Eisenberg, P.L. Cohen, and B.L. Kotzin. 1994. Development of the T cell receptor repertoire in lpr mice. *Semin. Immunol.* 6:19–26.

25. Jenkinson, E.J., R. Kingston, C.A. Smith, G.T. Williams, and J.J. Owen. 1989. Antigen-induced apoptosis in developing T cells: a mechanism for negative selection of the T cell receptor repertoire. *Eur. J. Immunol.* 19:2175–2177.

26. Huber, B.T. 1992. Mls superantigens: how retroviruses influence the expressed T cell receptor repertoire. *Semin. Immunol.* 4:313–318.

27. Ruberti, G., A. Gaur, C.G. Fathman, and A.M. Livingstone. 1991. The T cell receptor repertoire influences Vβ element usage in response to myoglobin. *J. Exp. Med.* 174:83–92.

28. Yamamoto, Y., K. Backlin, H. Nakagomi, E. Halapi, C. Juhlin, A. Bucht, and R. Kiessling. 1993. Cytotoxic activity and T cell receptor repertoire in tumor-infiltrating lymphocytes of adrenal cell carcinomas. *Cancer Immunol. Immunother.* 37:163–168.

29. Chang, H.C., A. Smolyar, R. Spoerl, T. Witte, Y. Yao, E.C. Goyarts, S.G. Nathenson, and E.L. Reinherz. 1997. Topology of T cell receptor-peptide/class I MHC interaction defined by charge reversal complementation and functional analysis. *J. Mol. Biol.* 271:278–293.

30. Fields, B.A., and R.A. Mariuzza. 1996. Structure and function of the T cell receptor: insights from X-ray crystallography. *Immunol. Today*. 17:330–336.

31. Bentley, G.A., G. Boulot, K. Karjalainen, and R.A. Mariuzza. 1995. Crystal structure of the β chain of a T cell antigen receptor. *Science*. 267:1984–1987.

32. Shoukry, N.H., P.M. Lavoie, J. Thibodeau, S. De Souza, and R.P. Sekaly. 1997. MHC class II-dependent peptide antigen versus superantigen presentation to T cells. *Hum. Immunol.* 54:194–201.

33. Kraig, E., J.L. Pierce, K.Z. Clarkin, N.E. Standifer, P. Currier, K.A. Wall, and A.J. Infante. 1996. Restricted T cell receptor repertoire for acetylcholine receptor in murine myasthenia gravis. *J. Neuroimmunol.* 71:87–95.

34. Miller, G.G., J.F. Hoy, L.J. Nell, and J.W. Thomas. 1988. Antigen processing and the human T cell receptor repertoire for insulin. *J. Immunol.* 141: 3293–3298.

35. Yang, Y., B. Charlton, A. Shimada, R. Dal Canto, and C.G. Fathman. 1996. Monoclonal T cells identified in early NOD islet infiltrates. *Immunity*. 4: 189–194.

36. Pantaleo, G., H. Soudeyns, J.F. Demarest, M. Vaccarezza, C. Graziosi, S. Paolucci, M. Daucher, O.J. Cohen, F. Denis, W.E. Biddison, R.P. Sekaly, and A.S. Fauci. 1997. Evidence for rapid disappearance of initially expanded HIV-specific CD8$^+$ T cell clones during primary HIV infection. *Proc. Natl. Acad. Sci. USA.* 94:9848–9853.

37. Auwaerter, P.G., G.D. Hussey, E.A. Goddard, J. Hughes, J.J. Ryon, P.M. Strebel, D. Beatty, and D.E. Griffin. 1996. Changes within T cell receptor Vβ subsets in infants following measles vaccination. *Clin. Immunol. Immunopath.* 79:163–170.

38. Reiner, S.L., Z.E. Wang, F. Hatam, P. Scott, and R.M. Locksley. 1993. TH1 and TH2 cell antigen receptors in experimental leishmaniasis. *Science.* 259:1457–1460.

39. Launois, P., I. Mallard, S. Pingel, K.G. Swihart, I. Xenarios, H. Acha-Orbea, H. Diggelmann, R.M. Locksley, H.R. MacDonald, and J.A. Louis. 1997. IL-4 rapidly produced by Vβ4Vβ8CD4$^+$ T cells instructs Th2 development and susceptibility to *Leishmania major* in BALB/c mice. *Immunity.* 6:541–549.

40. Gea-Banacloche, J.C., E.E. Weiskopf, C. Hallahan, J.C.L. Brnaldo de Quiros, M. Flanigan, J.M. Mican, J. Falloon, M. Baseler, R. Stevens, H.C. Lane, and M. Connors. 1998. Progression of human immunodeficiency virus disease is associated with increasing disruptions within the CD4$^+$ T cell receptor repertoire. *J. Infect. Dis.* 177:579– 585.

41. Smith, J.G., D.M. Magee, D.M. Williams, and J.R. Graybill. 1990. Tumor necrosis factor-α plays a role in host defense against *Histoplasma capsulatum*. *J. Infect. Dis.* 162:1349–1353.

42. Sypek, J.P., and D.J. Wyler. 1991. Antileishmanial defense in macrophages triggered by tumor necrosis factor expressed on CD4$^+$ T lymphocyte plasma membrane. *J. Exp. Med.* 174:755–760.